Temperature dependence of Raman scattering and soft modes in $TlTiOPO_4$

1990 J. Phys.: Condens. Matter 2 7555

(http://iopscience.iop.org/0953-8984/2/37/001)

J. Phys.: Condens. Matter **2** (1990) 7555–7568. Printed in the UK

Temperature dependence of Raman scattering and soft modes in $TlTiOPO_4$

R V Pisarev†, R Farhi‡, P Moch‡ and V I Voronkova§

† Joffe Physico-Technical Institute, USSR Academy of Sciences, Leningrad 194021, USSR

‡ Laboratoire des Propriétés Mécaniques et Thermodynamiques des Matériaux (CNRS) Université Paris-Nord, 93430-Villetaneuse, France

§ Physics Department, Moscow State University, Moscow, USSR

Received 13 February 1990, in final form 15 May 1990

Abstract. The Raman scattering of $TlTiOPO_4$ has been studied from 110 K up to above the ferroelectric-to-centrosymmetric phase transition at $T_c \simeq 850$ K. At low temperatures the analysis of the spectra includes the electrostatic interactions involved in the polar modes which are responsible for the variations in the frequencies and in the intensities as a function of the wavevector direction. Most of the non-polar (A_2) and polar (B_1, B_2 and A_1) modes among the 189 expected ones have been tabulated. The frequencies of the lines related to internal vibrations of the tetrahedral PO_4 groups do not significantly depend upon the temperature. On the contrary, a soft transverse mode belonging to the A_1 irreducible representation has been observed in the ferroelectric phase. The square of its frequency decreases linearly with the temperature and vanishes at T_c. This mode is connected with the Tl^+ motion but its coupling with internal TiO_6 modes is evidenced through the temperature variation of Raman lines at higher frequencies.

1. Introduction

Titanyl orthophosphates and related compounds have been the subject of increasing interest during the past few years. Because of its non-linear optical and electro-optical properties which have found important applications, potassium titanyl orthophosphate ($KTiOPO_4$) (KTP) is the best known member of this family. However, rubidium titanyl phosphate (RTP) and thallium titanyl phosphate (TTP) as well as some of the isomorphous compounds obtained by substitution show similar properties. They belong to the same polar space group $Pna2_1$ (C_{2v}^9), with 8 formula units per primitive cell [1]. Besides their pyroelectricity along the ***c*** axis, they show highly anisotropic temperature-dependent dielectric and conductivity properties [2, 3]. The conductivity is ionic and related to the motion of the cations (K^+, Rb^+ or Tl^+) along ***c***; it is thermally activated and significantly higher in KTP than in the two other compounds. The crystal structure of KTP-type ferroelectrics [1] is definitely different from those of well known ferroelectrics, but nevertheless it contains some structural elements typical of perovskite-type ferroelectrics $ATiO_3$ and order-disorder ferroelectrics of KH_2PO_4 type. As in perovskites, all Ti^{4+} ions of KTP-type crystals are inside oxygen octahedra but, contrary to perovskites, all octahedra are strongly distorted not only in the ferroelectric phase but presumably

also in the paraelectric phase. Strongly distorted oxygen octahedra exhibit an anomalously short (1.718 Å) and an anomalously long (2.161 Å) Ti–O bond in such a way that Ti–O–Ti chains involving these alternating bonds are observed along the ***c*** axis. The polar character partly derives from this arrangement, but the mobile cations responsible for the ionic conductivity may also play an important role in ferroelectric properties. As in KH_2PO_4-type ferroelectrics, the KTP structure contains tetrahedral PO_4 groups, but because of their good structural stability they do not substantially contribute to ferroelectric properties.

The published data on dielectric properties [2, 3] and on refractive index temperature variations [4] indicate that the phase transition to a centrosymmetric structure is of second-order character and occurs at 1207 K, 1062 K and 852 K for KTP, RTP and TTP, respectively. This second-order character contrasts with the first-order character of the ferroelectric transition in the perovskites $BaTiO_3$ and $PbTiO_3$ and in KH_2PO_4-type crystals. In KTP-type crystals, the transition has been suggested to be of displacive type [2] but its exact mechanism remains unknown and an uncertainty exists about the high-temperature crystal structure which has been asserted to be *Pnam* [3]. In this situation, the Raman study of the vibrational spectra and of their temperature dependence could be a useful tool in the understanding of the mechanism of the phase transition.

The work on TTP which is presented below is a part of a more extensive investigation concerning TTP, RTP and KTP which is now in progress. TTP has been chosen as the first compound studied because of its low transition temperature T_c, which makes a temperature-dependent study easier. Furthermore, its ionic conductivity is low, compared for instance with KTP, and does not seem to increase drastically in the vicinity of T_c; a quantitative study of the contribution of the conductivity to inelastic light scattering involves some experimental difficulties and it was useful as a first step to minimise this problem. Finally, Raman data concerning TTP do not exist, while results on KTP and, to a less extent, RTP, have been previously published [5–9]. In this paper we shall often refer to the rather extensive work of Kugel *et al* [7], which mainly concerns KTP at low temperatures and room temperature. Our own results on this compound, which will be published when the extension to the high-temperature study is completed, roughly agree with the measurements of Kugel *et al*, in spite of some discrepancies which are probably due to the method of analysing the electrostatic interaction of the polar modes.

As previously pointed out [5] and easily shown using a classical symmetry analysis, one expects 189 optical modes which are all Raman active in the ferroelectric structure. A complete detailed analysis of the phonon spectrum is probably hopeless and one is led to classify the modes as related to vibrations of specific atomic groups (PO_4, TiO_6) or to their relative motions; such an approach is itself rather convenient [7] but one has to keep in mind that this usual separation between external and internal modes is not really satisfactory in this case since some of the oxygen atoms belong to two different groups.

Finally, most of the modes are polar and, owing to the electrostatic interaction, the Raman spectrum depends not only on the light polarisation but also on the direction of the wavevector of the studied modes. Frequencies, intensities and selection rules are affected by the electrostatic effects and, except for well defined geometrical arrangements providing truly longitudinal or truly transverse modes, this interaction gives rise to a coupling between the bare modes belonging to different irreducible representations which would be derived neglecting these effects, resulting in modes of 'mixed' character. On the other hand, the Raman tensor contains new terms related to the second-order susceptibility, the high value of which makes these materials very interesting for optical applications.

2. Results and discussion

Single crystals of TTP have been grown using a flux method. These crystals which showed a good optical quality were cut in a rectangular parallelepiped shape with edges parallel to the $\boldsymbol{a}$, $\boldsymbol{b}$ and $\boldsymbol{c}$ axes which, for orthorhombic crystal classes, coincide with the principal axes of the ellipsoid of indices. The Raman spectra were recorded using a triple monochromator and an argon ion laser working at 488 or 514.5 nm. In most cases the resolution was better than 2 cm^{-1}, thus allowing a precision of about 0.3 cm^{-1} in the frequency determination. Both backward and 90° geometries were used, giving access to various directions of the light polarisations and of the phonon wavevector with respect to the crystallographic axes. It should be noted that the optical activity is not involved in our experimental arrangement since, for the *mm*2 class, the only non-vanishing component of the gyration pseudo-tensor is g_{xy} and consequently does not affect the light propagating along an orthorhombic axis. The temperature was monitored within about 2 K from 110 to 900 K using an appropriate cryostat or furnace. Low-temperature results were obtained using a commercially available gas exchange cryostat. The oven was designed by us and home-made. It consists of an alumina laboratory tube surrounded by a heating wire and a thermal insulator. Two lateral windows (small solid angle) and one end window (large solid angle) made of high-optical-quality silica were used for the illumination in 90° geometry and for the collection of the scattered light, respectively. A thermocouple provides the information for the PID temperature stabilisation of the heating power, and the resulting sample temperature is obtained from another calibrated thermocouple. In the high-temperature range, a significant but reversible increase in the optical absorption of the sample was observed, which was more pronounced for $\boldsymbol{E} \parallel z$ than for the two other polarisations. Consequently, the temperature dependence of the line intensities could not be precisely evaluated.

2.1. Low-temperature spectra

Some of the lines of the room-temperature spectra showed a complex structure which was resolved at 110 K where in most cases the experimental linewidth did not significantly exceed the instrumental resolution (1.2 cm^{-1}). The sharpening of the spectra obtained from cooling at 5 K did not allow us to observe any further line.

Neglecting the electrostatic effect, from the crystal structure it can be seen that all the optical modes are Raman active and are distributed as 47 A_1 (xx, yy, zz) plus 48 A_2 (xy) plus 47 B_1 (xz) plus 47 B_2 (yz) modes.

Owing to the electrostatic interactions, this analysis is no longer valid when the phonon wavevector is not parallel to one of the orthorhombic axes. More precisely, one still expects 48 A_2 (xy) non-polar modes which are not affected by the long-range electrostatic interactions, but the remaining modes mix together; following Born and Huang [10] and Shapiro and Axe [11], an eigenvector $\boldsymbol{f}$ resulting from this interaction is expressed in terms of the eigenvectors $\boldsymbol{e}_j$ of the dynamical matrix related to the short-range coupling as

$$\boldsymbol{f} = \sum_j a_j \boldsymbol{e}_j \tag{1}$$

where the a_j-values are solutions of the following set of linear homogeneous equations:

$$\sum_{j'} [(\Omega_j^2 - \omega^2)\delta_{jj'} + [\varepsilon^\infty(\boldsymbol{u})]^{-1}(\boldsymbol{u}\cdot\boldsymbol{M}_j)(\boldsymbol{u}\cdot\boldsymbol{M}_{j'})]a_{j'} = 0. \tag{2}$$

In the above equation, Ω_j is the frequency of the bare mode labelled by j. $\boldsymbol{M}_j$ is its

dielectric polarisation which, in the studied case of an orthorhombic crystal, is parallel to x, y, z for j belonging to B_1, B_2 or A_1 representations, respectively. u is a unit vector parallel to the propagation direction of the studied mode and $\varepsilon^{\infty}(u)$ is written as

$$\varepsilon^{\infty}(u) = \varepsilon_x^{\infty} u_x^2 + \varepsilon_y^{\infty} u_y^2 + \varepsilon_z^{\infty} u_z^2 \tag{3}$$

where $\varepsilon_\alpha^\infty$ stands for the high-frequency permittivity along the principal axis α (x, y or z). The eigenfrequencies ω are given through the vanishing of the determinant of the set of equations (2).

It immediately results from equation (2) that, for u parallel to an orthorhombic axis, the coupling concerns only bare modes belonging to the same irreducible representation. There are three sets of polar modes, which can be still labelled according to B_1, B_2 and A_1, but one of the sets refers to longitudinal modes with frequencies higher than the related 'bare' frequencies (B_1, B_2, A_1 for u parallel to x, y, z, respectively). The two remaining sets are transverse modes and their frequencies are simply the bare frequencies. In our experiments this corresponds to the back-scattering geometry.

Concerning our Raman studies using 90° geometry, they refer to a u-vector lying in a plane perpendicular to an orthorhombic axis. Thus the mixing concerns the two sets of modes for which M_j lies in this plane. For such 'oblique' modes, a convenient labelling would refer to two irreducible representations of the orthorhombic group. As an example, for incident and scattered light, respectively, parallel to x and y, u is in the (x, y) plane and, in addition to the 48 A_2 non-polar modes, one theoretically expects a set of 47 A_1 transverse modes at the bare frequencies, and a set of 94 B_1–B_2 oblique modes with modified frequencies.

Experimentally, because of the large number of modes involved in the studied crystal, a complete fit of the set of equations (2) for all of them cannot be obtained and we have then chosen to investigate mainly the transverse frequencies. However, in the case of a mode showing a bare frequency far from the neighbouring ones and weakly coupled to them, the frequency dispersion versus the wavevector direction approximately follows the relation

$$\omega^2 = \Omega_T^2 + (\Omega_L^2 - \Omega_T^2)\cos^2\theta \tag{4}$$

where θ is the angle between u and the dielectric polarisation M of the studied mode.

The Raman tensor of a polar mode contains an electronic contribution related to the electro-optic coefficients. In addition, the mixing of the bare modes resulting from equation (2) has to be taken into account. Finally, one obtains

$$\mathbf{R}_f = \sum_j a_j(\mathbf{R}_j^0 + \mathbf{R}_j^e). \tag{5}$$

The symmetry properties of $\mathbf{R}_j^0$ are not affected by the polar character and derive in the usual way from the irreducible representation corresponding to the mode j. The additional term $\mathbf{R}_j^e$ is related [11] to the electronic contribution of the electro-optic coefficients, to M_j and to the components of u; it vanishes for transverse modes ($u \cdot M_j = 0$).

From the above considerations, compared with the non-polar case, the Raman selection rules are modified through the mixing and through the electro-optic contribution. However, for C_{2v}, each effect leads to the same modifications in the symmetry of the resulting Raman tensor. Finally, for purely longitudinal modes, the Raman tensor shows the same symmetry properties as for purely transverse modes, but the intensities can markedly differ since electro-optic effects appear only for longitudinal modes.

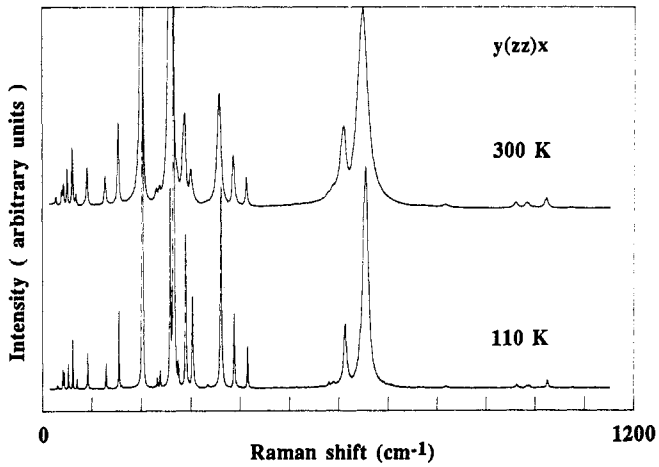

Figure 1. Comparison of the Raman spectra obtained in $y(zz)x$ geometry (A_1 transverse modes) at 300 and 110 K.

Experimentally, most of the spectra available according to the sample crystallographic orientations have been obtained. They allow a complete study of the A_2 modes and of the transverse B_1, B_2 and A_1 polar modes. Concerning the longitudinal vibrations the A_1 modes can be observed through the back-scattering geometry ($z(xx)\bar{z}$ and $z(yy)\bar{z}$ spectra), but there is no access for this case to the zz polarisation which, for most of the transverse A_1 lines, shows the highest intensity. Note that there is no way to observe directly longitudinal B_1 and B_2 lines. Because of the above-mentioned mixing effects on frequencies and selection rules, and the large number of interacting neighbouring modes, a detailed analysis of the 90° polarised Raman spectra involving oblique lines could not be achieved. However, in some cases the obliqueness was evidenced through a frequency shift as referred to the transverse line. The modification of the selection rules resulting from the mixing of oblique modes is more tedious to derive from the experimental spectra and was only qualitatively observed; for some lines, one polarisation is strongly dominant while, using other arrangements, the 2–3% polarisation leakage provides the main contribution to the experimentally measured intensity and in yet other cases the intensities are comparable in two distinct polarisations but the occurrence of accidental pseudo-degeneracies of bare modes in the vicinity of the measured frequency may obscure the situation.

We have compared in figure 1 the A_1 transverse modes in zz polarisation at 110 and 300 K. A_2, B_1 (transverse) and B_2 (transverse) spectra at 110 K have been represented in figures 2, 3 and 4 respectively, and figure 5 shows transverse and longitudinal A_1 modes in yy polarisation at the same temperature. The observed frequencies of the A_2 modes and of the transverse B_1, B_2 and A_1 modes are listed in table 1. In addition, the longitudinal A_1 frequencies have been reported and tentatively connected to their transverse parent. The intensity range extends over three orders of magnitude. As usual, and as previously noted for KTP and RTP [7], some modes are not observed. Conversely, owing to the combined effects of polarisation leakage and of pseudo-degeneracies, some identifications remain questionable; the corresponding frequencies have been given within parentheses.

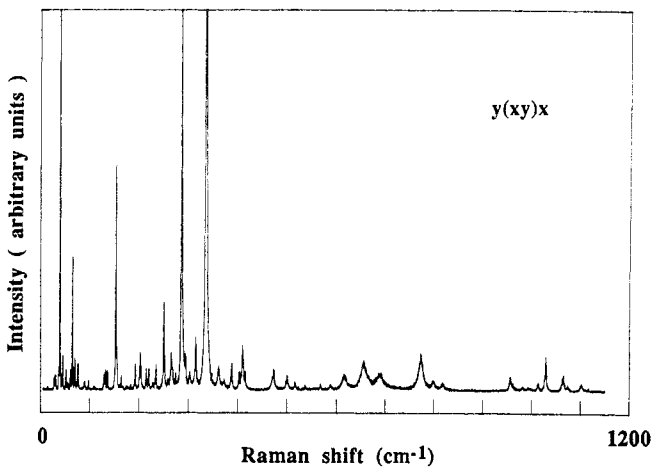

Figure 2. Raman spectrum obtained for the A_2 modes in $y(xy)x$ geometry at 110 K.

Concerning the comparison of longitudinal with transverse A_1 spectra, the observed frequency shifts are generally small or even negligible except for one line which shifts from 654.1 cm^{-1} (transverse) up to 736.3 cm^{-1} (longitudinal). This relatively well isolated mode is also easily identified in experimental conditions, providing an oblique conformation (namely $x(yy)z$) as shown in figure 6, and its frequency approximately obeys equation (4). There are no published results concerning infrared spectroscopy of TTP but it is evident that this mode corresponds to the A_1 mode observed in the reflectivity spectrum of KTP with 687 cm^{-1} transverse and 769 cm^{-1} longitudinal frequencies and reported at the intermediate value of 700 cm^{-1} in the Raman study [7]. From a more general point of view, the set of the observed longitudinal-to-transverse-frequency ratios for the A_1 modes provides a value for $\varepsilon_{33}^0/\varepsilon_{33}^\infty$ lying at around 2.5, assuming that the Lyddane–Sachs–Teller (LST) relationship is relevant.

The behaviour of the intensity versus the wavevector direction can be theoretically easily discussed for an isolated line, since from equation (2) the dielectric polarisation of such a mode should be proportional to $(\Omega_L^2 - \Omega_T^2)^{1/2}$. In the case of the above-mentioned 654 cm^{-1} (transverse)–736 cm^{-1} (longitudinal) A_1 line, the dielectric polarisation is the largest experimentally observed and it is then expected to induce the largest electro-optic contributions to the Raman tensor for the two observable components in the longitudinal geometry: $z(xx)\bar{z}$ and $z(yy)\bar{z}$, respectively. The intensities of the corresponding transverse lines, recorded in $y(xx)\bar{y}$ and $x(yy)\bar{x}$, respectively, are thus expected to differ from the longitudinal lines through these electro-optic terms of the Raman tensor. However, the experimental precision of the intensities of $z(yy)\bar{z}$ and $x(yy)\bar{x}$ spectra is rather poor since the sample has to be displaced between the two recordings, and the uncertainty is about 50%. Within this range the intensities of the above-mentioned lines are comparable.

Looking now at the intensity ratios of the longitudinal to transverse lines for the other well identified pairs, our experimental data show a rather large dispersion since they spread over more than one order of magnitude. As a result the overall aspect of the longitudinal and transverse spectra markedly differs from each other. The observed effects cannot be quantitatively analysed but, if we take into account the rather small

Table 1. Measured Raman frequencies at 110 K for A_2, transverse B_1, B_2, A_1 and longitudinal A_1 modes. The corresponding spectra have been obtained in $y(xy)x$, $y(zx)\bar{y}$, $x(zy)\bar{x}$, $y(zz)x$ and $z(yy)\bar{z}$ geometries respectively, except for A_1 (transverse) frequencies labelled with an asterisk, which have been measured using $x(yy)\bar{x}$ geometry. The frequencies of the A_1 longitudinal modes have been printed on the same line as their transverse parent.

ν (cm^{-1})				
A_2	B_1 (transverse)	B_2 (transverse)	A_1 (transverse)	A_1 (longitudinal)
28.8	26	27.3	30.7	31.0
31.0	30.4	37.7	41.3	41.7
39.7	(37.7)	52.7	43.9	44.7
45.7	51.9	69.2	44.9*	(51.9)
(52.5)	61.2	(89.0)	52.5	54.3
56.7	(69.9)	98.0	61.5	62.3
65.5	76.0	109.0	70.4	70.6
(70.4)	(89.0)	(129.2)	92.1	92.6
76.7	98.3	137.7	129.3	129.3
90.3	(129.2)	156.1	155.5	156.5
98.5	136.7	(164.5)	161.3	161.7
(129.2)	177.5	166.5	202.0	202.4
131.8	183.2	202.0	203.6	(207.5)
136.4	(203.6)	214.9	232.7	232.8
153.0	204.7	220.1	238.6	238.8
164.5	207.5	225.5	259.0	
192.8	(228.5)	(228.5)	265.9	(266.2)
(228.5)	(234.6)	234.4	274.5	
234.6	244.6	238.6	289.8	289.8
250.6	252.9	263.6	303.6	
286.4	270.0	282.7	314.9*	(317.0)
294.1	288.3	302.0	334.3	(337.5)
315.6	295.3	316.7	(335.7)*	
336.3	309.5	327.6	361.6	361.8
(403.8)	311.6	(341.0)	373.3*	
410.4	335.7	362.6	388.5	388.6
472.8	397.2	374.4	415.6	
500.4	408.0	383.9	469.0*	(482.0)
516.0	416.9	403.8	515.2	516.3
536.3	471.7	409.1	544.6*	545.6
567.2	481.1	472.5	567.9*	568.1
588.0	492.1	552.1	580.0	582.2
(656.1)	557.5	561.2	588.6	588.8
774.4	586.3	587.0	613.0	614.5
800.2	614.6	616.7	654.1	736.3
818.9	(656.1)	(656.1)	818.0	818.8
956.7	699.3	817.3	935.0	
1013.7	766.4	959.4	962.3	962.6
1029.0	796.9	980.6	983.7	984.2
1064.7	(818.9)	996.5	987.8	987.8
1074.4	960.4	999.6	998.8*	1000.3
1102.0	984.8	1022.7	1013.3*	(1020.5)
	995.1	(1075.3)	1025.3	
	1023.8	1079.9	1074.9	(1074.9)
	1075.7	1106.2		

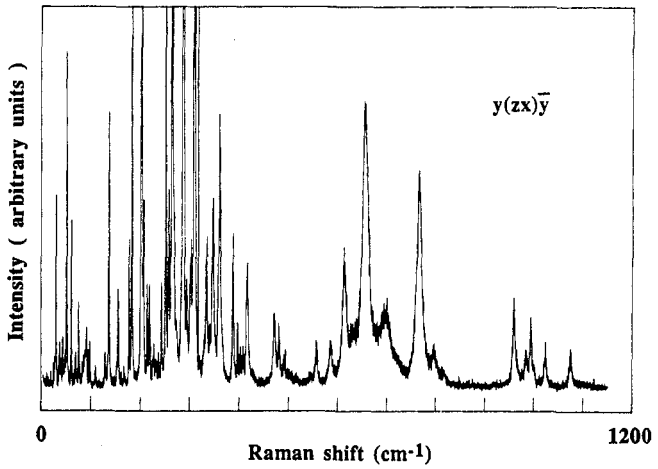

Figure 3. Raman spectrum obtained for the B_1 transverse modes in $y(zx)\bar{y}$ geometry at 110 K.

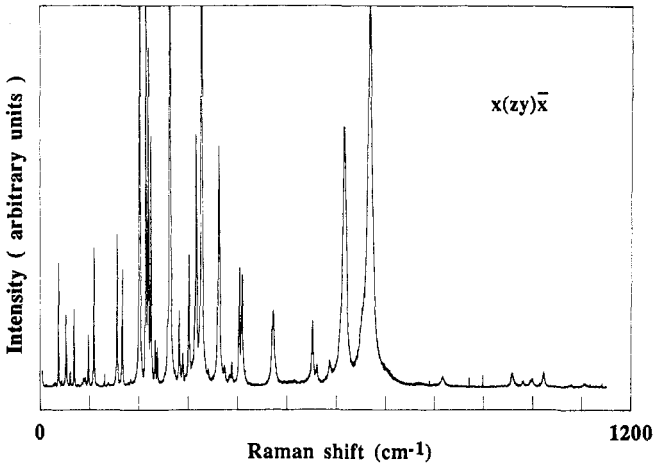

Figure 4. Raman spectrum obtained for the B_2 transverse modes in $x(zy)\bar{x}$ geometry at 110 K.

observed frequency shifts—except for the line at $\Omega_T = 654.1\ cm^{-1}$—their magnitude seems to exceed the predictions of the model summarised above.

The above-described intensity and frequency variations are likely to explain some discrepancies between previously reported results on KTP [5–9] and between these results and our own unpublished measurements on this compound.

In the case of the A_2 non-polar modes, our experimental spectra do not depend on the direction of light propagation, as expected, since the above considerations are irrelevant.

The high-frequency Raman spectra of TTP and KTP show strong similarities and, as shown in figure 7, for frequencies higher than about $150\ cm^{-1}$ most of the lines appear in both spectra with differences in frequencies not exceeding a few tens of reciprocal centimetres. An attempt to analyse the high-frequency spectrum in relation with the

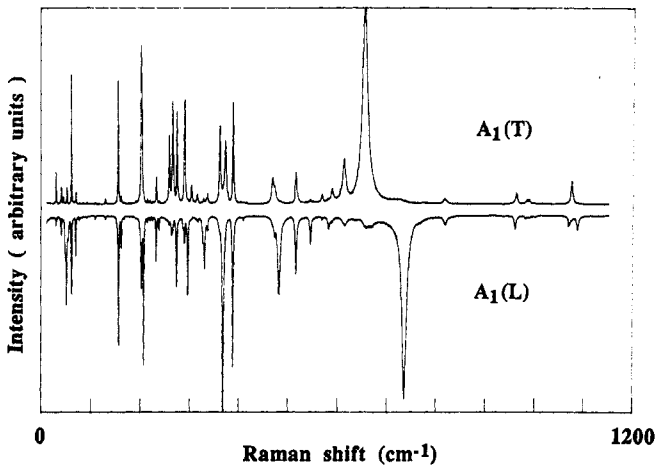

Figure 5. Raman spectra obtained for the A_1 (transverse) and A_1 (longitudinal) modes at 110 K. The intensity scale for the longitudinal modes has been reversed to make the comparison easier.

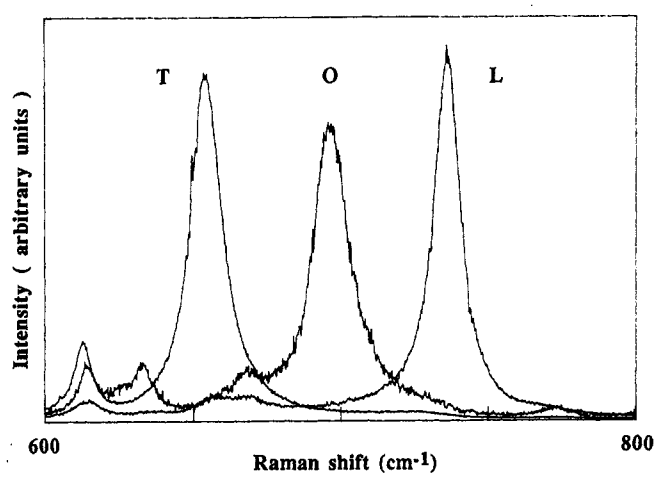

Figure 6. Raman spectra of the A_1 mode submitted to the most important longitudinal transverse splitting (normalised intensities). (T: transverse; L: longitudinal; O: oblique.)

internal modes of the PO_4 tetrahedra and of the TiO_6 octahedra was made by Kugel *et al* [7]. Roughly speaking, between 200 and 350 cm^{-1} and between 600 and 800 cm^{-1} the assignments concern the TiO_6 octahedra [$\nu_4(F_{1u})$, $\nu_5(F_{2g})$, $\nu_6(F_{2u})$] and [$\nu_1(A_{1g})$, $\nu_2(E_g)$, $\nu_3(F_{1u})$], respectively. Between 350 and 600 cm^{-1} and above 800 cm^{-1}, the observed Raman lines are attributed to vibrations of the PO_4 tetrahedra, [$\nu_2(E)$, $\nu_4(F_2)$] and [$\nu_1(A_1)$, $\nu_3(F_2)$], respectively. Such an approach which, as mentioned in section 1, can be justified only partially owing to interactions between the above species through a common oxygen atom, is supported by the values of the measured frequencies and, in the case of TTP, by the temperature dependence of the spectra as discussed in the next section. In the spirit of this analysis, the modes below 200 cm^{-1} have to be thought of as

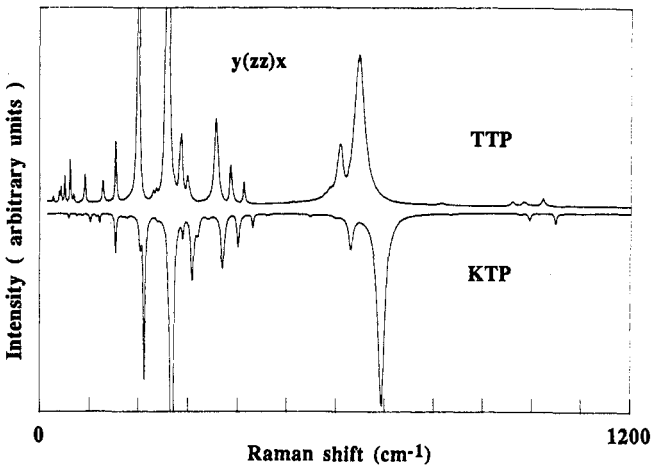

Figure 7. Raman spectra recorded in $y(zz)x$ geometry at 300 K for TTP and KTP. The intensity scale for KTP has been reversed to make the comparison easier.

external modes. This is not in doubt for the lowest-frequency lines, which are assumed to be mainly related to the monovalent ion translations; for KTP our lowest measured frequency lies at 58 cm^{-1} at 300 K (in agreement with earlier published work [5, 6, 8]) while for TTP it is at 27.7 cm^{-1} at the same temperature. Such a large difference mainly derives from the ratio of the masses of Tl to K which is equal to 5.2 and would lead to a frequency ratio of about 2.3. Such a picture ignores the motion of the other ions and the modifications of the potential induced by the replacement of the cation in the crystal, but it gives a rough estimation to compare with the experimental value of 2.1.

2.2. Temperature dependence and soft mode

Above the transition temperature T_c ($\simeq$ 850 K), the Raman spectra of TTP do not allow us to derive much conclusive information. Except for a few lines in the low-frequency range, when temperature has been increased, one observes severe broadening (figure 8) which, above 800 K, leads to weakly resolved scattering. As a result, no attempt was made to connect the spectra above T_c to the crystal structure in the high-temperature range. We only noticed that below T_c the intensity of the polar modes significantly decreases at high temperatures, and above T_c the scattering in the zz, zx and zy polarisations becomes very weak while it remains approximately constant in the xy polarisation. However, the quantitative measurements are very poor since, when maintained at a high temperature, the samples are subject to a drastic decrease in their optical quality owing to defects created in the crystals. Consequently we obtained only a limited number of Raman spectra above T_c, and we have restricted our investigation to temperatures lower than about 870 K.

Fortunately, the Raman spectra begin to be affected well below 850 K and, as discussed hereafter, their variation is, at least partly, related to the phase transition. Most of the spectra were recorded using a 90° geometry which was the most easily accessible at high temperatures. Our discussion mainly concerns spectra with incident and scattered light propagations parallel to y and x, respectively, allowing us to observe

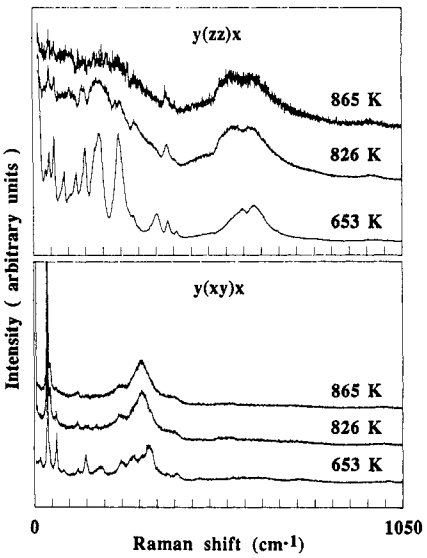

Figure 8. High-temperature Raman spectra obtained in $y(zz)x$ and $y(xy)x$ geometries at 653, 826 and 865 K.

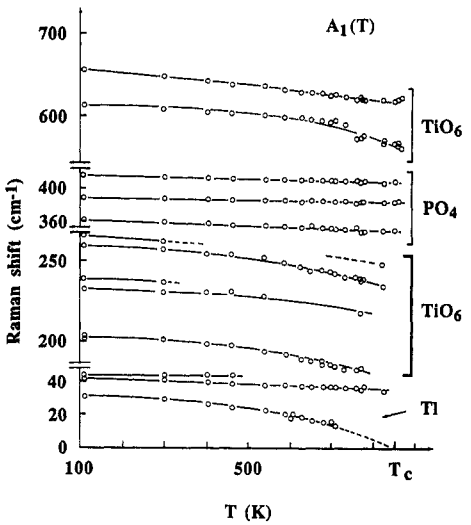

Figure 9. Frequency versus temperature variations of selected Raman lines recorded in $y(zz)x$ geometry (pure A_1 transverse modes). The lines are guides for the eye.

the A_2 non-polar modes (xy) and the A_1 transverse modes (zz) while (xz) and (zy) spectra are connected with the B_1–B_2 oblique modes.

In addition to the above-mentioned broadening and intensity decreases, in the high-frequency range (above 150 cm^{-1}) the lines related to the PO_4 internal modes do not show significant frequency variations, while those connected with the TiO_6 internal modes present a more or less pronounced softening of a few tens of reciprocal centimetres between 300 and 800 K for polar modes. In xy polarisation, for many lines, the weak intensity of the spectra prevents any detailed analysis. We have reported in figure 9 the temperature variations in the frequencies of some of the PO_4 and TiO_6 internal modes of A_1 (transverse) symmetry, and in figure 10 those of B_1–B_2 mixed modes obtained from (zx) and/or (yz) spectra.

The most characteristic features are observed in the low-frequency spectrum, and more specifically below 50 cm^{-1}. As mentioned above, it mainly concerns the Tl^+ translations. In the (zz) geometry (figure 9), one line at 29 cm^{-1} for $T = 300$ K softens down to below 15 cm^{-1} at 700 K. Some significant spectra are given in figure 11. This line cannot be followed above 700 K since we also observe a very broad band of scattered light centred at zero frequency (figure 8) which prevents measurements at low frequencies. However, in the 300–700 K range, the square of its wavenumber shows a linear dependence on temperature with a slope of about -1.45 cm^{-2} K^{-1} (figure 12) and extrapolates to zero at $T \simeq T_c$. This behaviour fits the standard model fairly well for a displacive phase transition monitored by a soft-phonon mode. In KTP, a similar hypothesis has been previously suggested through the study of the unpolarised Raman spectrum as a function of the pressure [6] (but not temperature); a soft mode (at 56 cm^{-1} for 1 atm) appears in the spectrum and the identification of this line should be related to the temperature-dependent line reported here for TTP. However, as will be discussed elsewhere, we have found that the temperature dependence of the KTP line strongly differs

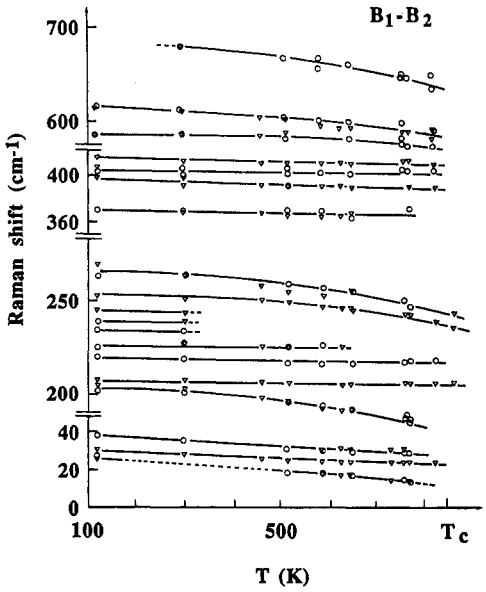

Figure 10. Frequency versus temperature variations of selected Raman lines recorded in xz (▽) and zy (○) polarisations. At 110 K, they correspond to pure B_1 and B_2 transverse modes, respectively, while at higher temperatures, because of the 90° geometry used, the modes are oblique and possibly mixed (see text). The lines are guides for the eye.

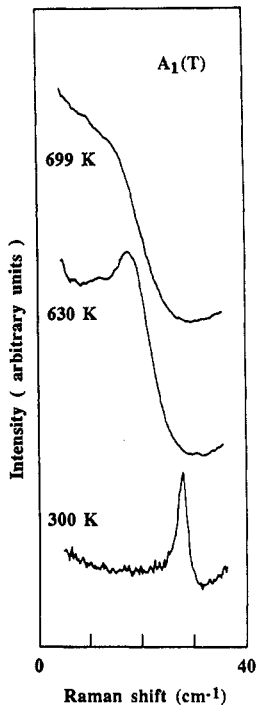

Figure 11. Selected Raman spectra of the soft A_1 (transverse) mode recorded in the $x(zz)y$ geometry.

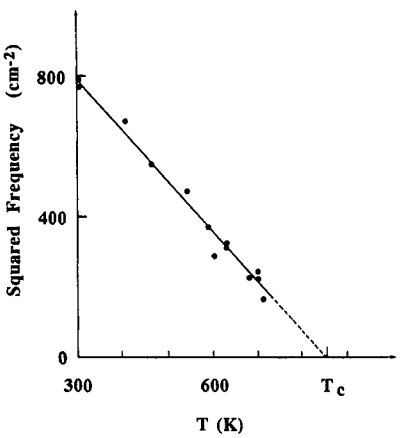

Figure 12. The squared frequency of the soft mode as a function of the temperature.

from the simple behaviour observed for TTP, and this is probably related to a strong coupling for KTP of the soft mode with a diffusive mode related to the rather high ionic conductivity in this compound at high temperatures. Such a diffusive mode is also detected for TTP and prevents, as already mentioned, the observation of low-frequency phonon lines at a temperature above 700 K.

From the results just discussed, TTP could be considered as a candidate for an archetypal example where the phase transition is driven by the softening of one low-frequency mode. It should be noted that the inverse dielectric permittivity $(\varepsilon_{33}^0)^{-1}$ obeys a Curie–Weiss law below T_c [2], in agreement with the LST relationship assuming that the squared frequency of one transverse mode softens linearly with temperature. Nevertheless the LST relation could not be quantitatively verified since no information has been obtained about the behaviour of the longitudinal modes as a function of temperature.

The temperature variations in the high-frequency lines are to be interpreted in terms of mode coupling. However, apparently the nature of the symmetries of the coupled modes does not play a major part, in contrast with the theoretical predictions and with most of the experimental examples. Anyway, it is important to note that the concerned modes are related to the TiO_6 internal vibrations. This supports the hypothesis that both Tl^+ ions and TiO_6 octahedra are involved in the ferroelectric transition of TTP.

To conclude the discussion of the low-frequency behaviour, we have also observed significant softenings in the other spectra. Nevertheless, the (xy) spectrum low-frequency line can by no means be extrapolated to zero at around 850 K, and the analysis of the B_1–B_2 spectra cannot be easily performed since the mixing effects appear to be temperature dependent; not only the frequency but also the intensity of the polarised lines strongly vary and it is difficult to follow the temperature variation of a given line. In the (xy) spectra we observe, at any temperature and even above the phase transition, a sharp Raman line the frequency of which hardly changes with temperature (39.5 cm^{-1} at 300 K; 38 cm^{-1} at 865 K). This behaviour contrasts with all the other observed features in the Raman spectra and we could not find any explanation for it.

3. Conclusion

It has been shown that some features of the temperature dependence of the Raman scattering of TTP can be interpreted in connection with the phase transition at $T_c \simeq$ 850 K. In the non-centrosymmetric C_{2v} phase below T_c, the polar character of most of the Raman active modes has to be carefully taken into account in order to obtain significant results, and a detailed study at low temperatures has been performed, in which the polarisations as well as the directions of incident and scattered light were suitably varied. We have thus been able to tabulate most of the non-polar (A_2) and polar (B_1, B_2 and A_1) modes expected from group theoretical considerations and, for the polar modes, to study the frequency and intensity variations of the polarised spectra in relation to the wavevector direction of the involved phonon. In fact, such effects have been previously reported in the literature, but they generally concern crystals with a small number of atoms per unit cell which consequently provide only a few Raman lines in contrast with the complicated structures exhibited by titanyl phosphates. Up to now, in the published work concerning Raman scattering of KTP and RTP, only minor attention has been paid to these polar effects and this hinders comparison between the available experimental results and their dependence upon an intentionally varied parameter (composition, temperature or pressure). Our low-temperature measurements did not

allow us to derive all the quantities needed for the identification of the motions and of the polarisability of each Raman line but provided us with information necessary in order to start the temperature dependence measurements. On the other hand, following Kugel *et al* [7], we were able to connect most of the Raman lines to pseudo-internal PO_4 and TiO_6 modes or to external modes. In this last case, some low-frequency lines appeared to be closely related to the Tl^+ cation motions. Concerning the temperature variation, the main result consists of a Raman line the squared frequency of which extrapolates to zero at T_c. It corresponds to a transverse mode belonging to the A_1 representation as expected when referring to a Landau model for a displacive second-order phase transition and is mainly connected with the Tl^+ motion. A moderate softening of the TiO_6 internal modes is also observed, presumably indicating a coupling to the soft low-frequency mode which, at first glance, monitors the transition. This supports the previously reported hypothesis assuming that both Tl^+ ions and TiO_6 octahedra play a significant part in the phase transition and in the pyroelectric properties, but a quantitative analysis would require additional information on the crystal structure above T_c which, unfortunately, cannot be derived from the high-temperature Raman spectra. In any case, some other features mentioned in the preceding section show that a too naive model dealing with one soft mode for a displacive phase transition provides a rather crude scheme compared with the experimental reality.

Contrary to the above-mentioned behaviour, the modes related to internal vibrations of PO_4 tetrahedra, as well as some of the low-frequency external modes, do not show any pronounced softening over a very large temperature range from 110 K up to the phase transition.

Finally a comparative study of TTP, RTP and KTP which is now in progress shows that the ionic conductivity has also to be taken into account.

References

[1] Tordjman I, Masse R and Guitel J C 1974 *Z. Kristallogr.* **139** 103
[2] Yanovskii V K and Voronkova V I 1980 *Phys. Status Solidi* a **93** 665
[3] Yanovskii V K, Voronkova V I, Leonov A P and Stefanovitch S Yu 1985 *Sov. Phys.–Solid State* **27** 1508
[4] Pisarev R V, Markovin P A, Shermatov B N, Voronkova V I and Yanovskii V K *4th Jpn–Sov. Symp. on Ferroelectrics (Tsukuba, August 1988); Ferroelectrics* at press
[5] Garmash V M, Govorun D N, Korotkov P A, Obukhovskii V V, Pavlova N I and Rez I S 1985 *Opt. Spectrosc.* **58** 424
[6] Kourouklis G A, Jayaraman A and Ballman A A 1987 *Solid State Commun.* **62** 379
[7] Kugel G E, Bréhat F, Wyncke B, Fontana M D, Marnier G, Carabatos-Nedelec C and Mangin J 1988 *J. Phys. C: Solid State Phys.* **21** 5565
[8] Kugel G E, Mohamadou B and Marnier G *7th Int. Meet. on Ferroelectricity (Saarbrücken, 1989); Ferroelectrics* at press
[9] Xu L W, Chang D W, Niu H D and Jia Sh Q 1989 *Chinese Phys. Lett.* **6** 225
[10] Born M and Huang K 1968 *Dynamical Theory of Crystal Lattices* (Oxford: Clarendon) p 265
[11] Shapiro S M and Axe J D 1972 *Phys. Rev.* B **6** 2420